Solid Earth Discuss., 5, 1659–1686, 2013
www.solid-earth-discuss.net/5/1659/2013/
doi:10.5194/sed-5-1659-2013

Solid Earth
Discussions
Open Access

Seismogenic frictional melting in the magmatic column

J. E. Kendrick[1,2], Y. Lavallée[1], K.-U. Hess[2], S. De Angelis[1], A. Ferk[2,3], H. E. Gaunt[4], D. B. Dingwell[2], and R. Leonhardt[3]

[1]School of Earth, Ocean and Ecological Sciences, Liverpool, L69 3GP, University of Liverpool, UK
[2]Department of Earth and Environmental Sciences, Ludwig-Maximilians-Universität, Theresienstr. 41, 80333 Munich, Germany
[3]Central Institute for Meteorology and Geodynamics, 1190 Vienna, Austria
[4]Rock & Ice Physics Laboratory, Department of Earth Sciences, University College London, Gower Street, London, UK

Received: 18 September 2013 – Accepted: 25 September 2013 – Published: 16 October 2013

Correspondence to: J. E. Kendrick (jackie.kendrick@liverpool.ac.uk)

Published by Copernicus Publications on behalf of the European Geosciences Union.

Abstract

Lava dome eruptions subjected to high extrusion rates commonly evolve from endogenous to exogenous growth and limits to their structural stability hold catastrophic potential as explosive eruption triggers. In the conduit, strain localisation in magma, accompanied by seismogenic failure, marks the onset of brittle magma ascent dynamics. The rock record of exogenous dome structures preserves vestiges of cataclastic processes (Cashman et al., 2008; Kennedy and Russell, 2011) and of thermal anomalies (Kendrick et al., 2012), key to unravelling subsurface processes. Here, a combined structural, thermal and magnetic investigation of a shear band crosscutting a large block erupted in 2010 at Soufrière Hills volcano (SHV) reveals evidence of faulting and frictional melting within the magmatic column. The mineralogy of this pseudotachylyte vein offers confirmation of complete recrystallisation with an isothermal remanent magnetisation signature that typifies local electric currents in faults. The pseudotachylyte presents an impermeable barrier, which is thought to have influenced the degassing pathway. Such melting events may be linked to the step-wise extrusion of magma accompanied by repetitive long-period (LP) drumbeat seismicity at SHV (Neuberg et al., 2006). Frictional melting of SHV andesite in a high velocity rotary shear apparatus highlights the small slip distances (< 15 cm) required to bring 800 °C magma to melting point at upper conduit stress conditions (10 MPa). We conclude that frictional melting is an inevitable consequence of seismogenic, conduit-dwelling magma fracture during dome building eruptions and that it may have an important influence on magma ascent dynamics.

1 Background

Dome-building eruptions hold potential for volcanic catastrophes, with dome collapse leading to devastating pyroclastic flows with almost no warning (Carn et al., 2004; Herd et al., 2005; Voight and Elsworth, 2000). Extrusion of high-viscosity magma at

SED
5, 1659–1686, 2013

arc volcanoes is frequently accompanied by seismic activity in the form of repetitive drumbeat, LP events (De Angelis, 2009; Iverson et al., 2006; Neuberg et al., 2006). At SHV this seismicity has been attributed to cyclic plug extrusion dictated by magma supply rate, conduit geometry (Rowe et al., 2004), overpressure build-up (Edmonds and Herd, 2007; Lensky et al., 2008), rheological stiffening (Voight et al., 1999) and magma fracture (De Angelis and Henton, 2011). During magma ascent at SHV crystal growth suppresses the thermal runaway due to viscous heating and so the magma temperature remains close to that of the magma chamber (Hale et al., 2007), which has been estimated at 830–858 °C (Devine et al., 1998; Melnik and Sparks, 2002; Murphy et al., 2000) up to 880 °C when heated by an incoming mafic intrusion (Barclay et al., 1998; Devine et al., 1998). Magma column heterogeneity develops in crystalline magmas as areas of dense magma are surrounded by shear zones at the conduit margin (Hale and Wadge, 2008; Kendrick et al., 2012, 2013; Lavallée et al., 2012b), which can ultimately result in stick-slip behaviour as observed at SHV (Neuberg et al., 2006). At this point the driving forces of the buoyant magma are superseded by frictional controls along the conduit margin (Lavallée et al., 2012a); where brittle fracture and sliding can lead to formation of gouge, cataclasite (Cashman et al., 2008; Kennedy et al., 2009) and pseudotachylyte (Kendrick et al., 2012) akin to tectonic fault zones (Curewitz and Karson, 1999; Kirkpatrick and Rowe, 2013; Lin, 1996). Frequent transitions from explosive to effusive behaviour, partially driven by the development of the degassing network at SHV, may have been governed by the formation of shear zones (Carn et al., 2004; Plail et al., 2013; Watts et al., 2002). Hence, faulting and subsequent slip of ascending magma (Cordonnier et al., 2012; De Angelis and Henton, 2011; Kendrick et al., 2013; Lavallée et al., 2008; Tuffen and Dingwell, 2005) is of critical importance to the explosivity of volcanic eruptions (Castro et al., 2012; Lavallée et al., 2013; Okumura et al., 2010).

SED
5, 1659–1686, 2013

2 Analytical investigation

2.1 Petrology and petrography

Meter-scale blocks from block-and-ash flow deposits at SHV present the opportunity to study textural and structural information from conduit and dome material that would otherwise remain inaccessible due to the current volcanic unrest. Of specific interest is a ~ 2 m long shear band located in an andesitic block erupted in 2010 due to its vitreous appearance, lateral extent and structural signature. The shear band cross-cuts the centre of its meter-scale host rock, which confirms its origin within the magmatic column. This is in stark contrast to frictional marks on the surface of blocks formed during turbulent flow of pyroclastics at SHV (Grunewald et al., 2000). The shear band consists of interlayered aphanitic pseudotachylyte and granular cataclasite up to 3 cm thick which pinches out, widens and bends along length (~ 2 m) and breadth (Figs. 1 and 2), demonstrating post-formation ductile deformation in the still-flowing, conduit-dwelling, magma. The host rock, a porphyritic andesite, has a crystal assemblage of plagioclase, amphibole and orthopyroxene phenocrysts, with some quartz grains and FeTi oxide (total crystallinity < 60 %) set in a groundmass of clinopyroxene, orthopyroxene and plagioclase (Figs. 3a and 4). There are 2 types of plagioclase, categorised as having < An80 (type 1) or > An80 (type 2). Type 1 is more common and is present across the sample whereas type 2 tends to form as rims and is only present in the host rock (Fig. 4). Amphiboles are broken down into pseudomorphs containing plagioclase, pyroxene and abundant FeTi oxides as has been reported from earlier in the eruption (Zellmer et al., 2003). These could result from dehydration reactions of amphibole during ascent or from long repose intervals in the conduit, as well as from late-stage oxidation to form opacite (Garcia and Jacobson, 1979; Murphy et al., 2000), which is common in this sample. What interstitial glass may have existed is fully devitrified; which could indicate prolonged residence times (Baxter et al., 1999). The glass has been replaced by silica residue, including feldspar and cristobalite, probably through high-temperature vapour-phase reactions along degassing pathways in the conduit

SED
5, 1659–1686, 2013

(Baxter et al., 1999; Horwell et al., 2010, 2013). In earlier stages of the eruption silica polymorphs, including cristobalite, have comprised up to 15 wt. %. Its presence here was verified using differential scanning calorimetry (DSC) (Fig. 5).

High sensitivity (HS)-DSC measurements on the host rock groundmass revealed a reversible endothermic peak at 190 °C at a heating/cooling rate of 10 °C s^{-1}, which recurred after cooling and reheating, verifying the phase transition. While the ideal $\alpha-\beta$ phase transition of cristobalite occurs at 272 °C, highly distorted crystals originating from a gel or glass can have a lower transition temperature, and inversion temperatures of 120–272 °C have been recorded (Sosman, 1965).

The shear band reveals no such endothermic peak as a result of cristobalite, despite it being visible in thin section (Fig. 3b), however, a repeatable endothermic peak at 572 °C (Fig. 5) can be attributed to the $\alpha-\beta$ phase transition of quartz (Sosman, 1965). The relative abundance of the silica polymorphs in the vein vs. host rock (Fig. 4) account for the detection of the phase transitions by HS-DSC. The melting temperature of the shear zone also differs from the host rock; low sensitivity (LS)-DSC measurements on the groundmass of the host rock (phenocrysts are excluded from this measurement, removing amphibole from the reaction and thus somewhat increasing the melting temperature from that of the bulk sample) show two broad melting peaks between 1050–1250 °C and 1350–1450 °C (post optical analysis of samples after runs to 1300 and 1500 °C indicate partial and complete melting of all phases respectively) whereas the aphanitic pseudotachylyte vein shows a broad melting peak between 1200–1400 °C (post optical analysis indicates complete melting of all phases). This difference arises from the distinct mineralogy formed during disparate crystallisation histories (Fig. 4). In contrast to the host rock groundmass (Fig. 3a) the pseudotachylyte consists of fine grained (10–40 µm), equant and well sorted quartz, plagioclase, FeTi oxides, pyroxene, feldspar, cristobalite and cordierite (Fig. 3b), and occasional larger sieve-textured plagioclase phenocrysts (Fig. 3d). The mineral assemblage of the interlayered cataclasites is a combination of the pseudotachylyte and host rock (Figs. 3 and 4). The interlayered pseudotachylyte and cataclasite indicate repeat slip events along the fault

SED
5, 1659–1686, 2013

surface, hence cataclasites are granular aggregates of both starting material and pseudotachylyte (which contain grains up to several mm in diameter, although more typically 20–400 µm), as is frequently observed in tectonic fault zones (Kim et al., 2010; Kirkpatrick and Rowe, 2013; Rowe et al., 2005).

2.2 Magnetic anomalies

Crystallisation in the volcanic pseudotachylyte vein recorded a distinct magnetic signature, as is often noted in tectonic and impact generated pseudotachylytes (Ferré et al., 2005; Freund et al., 2007), which confirms its status as a frictionally generated melt. The remanence of the pseudotachylyte is carried by a low coercive material with a Curie temperature of 320 °C, whereas the host rock, which also shows low coercive behaviour, has two Curie temperatures at 400 and 540 °C. Alternating field demagnetisation of different remanent magnetisations was used to identify further differences between the two samples (Fig. 6). The remanence of the pseudotachylyte is comparable to an isothermal remanent magnetisation (IRM) which is typical of thermal anomalies, whereas the remanence of the host rock displays similarities to an anhysteretic remanent magnetisation. Thus, the pseudotachylyte has seen a strong magnetic field that overwrote the previous thermoremanent magnetisation of the magma. Due to the close proximity of the two samples (within 2 cm) this IRM cannot originate from a lightning strike (known to enforce magnetisation) but instead demonstrates its frictional melt origin, as high local electric currents occurring in a faults give rise to a strong IRM (Ferré et al., 2005; Freund et al., 2007).

3 Frictional melting in the conduit

The drastic contrast in mineralogical assemblage and petrographic textures (Figs. 2–4, and 7) between host rock and pseudotachylyte vein suggest that it formed due to localised melting of the host rock during faulting and frictional slip of the viscous

SED
5, 1659–1686, 2013

magma. The metastable melt was then able to crystallise slowly due to the high volcanic geotherm, forming the crystalline pseudotachylyte vein, with fine-grained, equant crystals (Figs. 3b and 4). This accounts for the very low porosity of the pseudotachylyte layers (1 %) as compared to the cataclasite in the shear band (15 %) or the host rock (23 %) (determined via helium pycnometry) depicted in the 3-D solid and pore-space reconstructions in Fig. 8. The pseudotachylyte is also up to three orders of magnitude less permeable than the host rock when perpendicular to flow direction (Fig. 9). The presence of chlorite (Fig. 4 d) suggests that the shear zone was involved in degassing (Plail et al., 2013), which would be channelled by the pseudotachylyte layer before the permeable porous network shuts off by complete crystallisation. Hence, when pseudotachylyte forms as part of a shear band this will significantly influence the efficiency of the degassing network, and may prove integral to explosive-effusive transitions (Castro et al., 2012; Edmonds and Herd, 2007).

The melting and recrystallisation of the magma locked-in a distinct thermal history, unravelled here using DSC. Contrasting melting temperatures of the pseudotachylyte vs. its host rock, and the occurrence of different phase changes during heating and cooling of the sample subsets confirm their divergent pasts, confirming the thermal anomaly. Finally, the disparate magnetic signature of the vein and host rock, resulting from high electric currents during faulting and frictional slip, solidifies its pseudotachylyte status. Indeed the demagnetisation experiments performed provide some of the clearest evidence to distinguish between pseudotachylyte and host rock (Ferré et al., 2005; Freund et al., 2007), which may be of use in other volcanic scenarios.

4 The mechanics of slip

Pseudotachylyte has previously been linked to seismogenic ruptures (Magloughlin and Spray, 1992) at slip velocities over $0.1\,m\,s^{-1}$ (Spray, 2010). Pseudotachylyte generation at SHV may be linked to the recorded repetitive drumbeat seismicity (Luckett et al., 2008; Neuberg et al., 1998; Rowe et al., 2004; Watts et al., 2002) inferred to

SED
5, 1659–1686, 2013

result from magma failure and stick-slip events along conduit margins (De Angelis and Henton, 2011; Harrington and Brodsky, 2007; Neuberg et al., 2006). LP events occur at approximately 50 s intervals with a *P* wave pulse duration of approximately 0.15 s (Fig. 10), which translates to a source duration of the same timeframe (Harrington and Brodsky, 2009). In order to calculate the displacement during these events we average the cumulative source displacement over 24 h, for example 235 m preceding the 29 July 2008 dome collapse (De Angelis, 2009) divided by the 1588 recorded events (of similar size) during that period to provide a mean slip distance of 15 cm per event. Together, this provides a slip velocity of 1.0 m s^{-1} for 15 cm in 0.15 s. To assess the effect of such slip conditions on the SHV andesite, we performed a high-velocity rotary shear experiment using an axial load (10 MPa) representative of approximately 500 m depth in the upper conduit. In this experiment two 25 mm diameter hollow cores (9.5 mm holes) were brought into contact and the axial load was applied. Next, one side was rotated at a velocity of 1.0 m s^{-1} as the simulated fault was recorded by optical and thermal videos to track the temperature profile and observe melting (see Hirose and Shimamoto (2005) for more details of methodology; see Supplement). When considering a minimum starting magma temperature of 800 °C (Barclay et al., 1998; Devine et al., 1998; Hale et al., 2007; Melnik and Sparks, 2002; Murphy et al., 2000), these slip conditions are more than enough to force the andesite through the amphibole stability field at 855 °C (Rutherford and Devine, 2003) and on into frictional melting above 950 °C (Fig. 11 and Supplement). Frictional melting may have important implications for eruption dynamics (Hale and Wadge, 2008), and because the frictional properties of melt differ greatly from gouge (Magloughlin and Spray, 1992; Spray, 2010), the consequence of frictional melting and viscosity-controlled slip dynamics may differ significantly from those anticipated from gouge-hosting, cataclastic shear zones frequently envisaged at conduit margins.

SED
5, 1659–1686, 2013

5 Conclusions

This study documents unequivocal evidence of frictional melting in ascending, conduit-dwelling magma. The presence of pseudotachylyte is verified using a multi-parmetric approach that assesses its structural and mineralogical character as well as its distinct thermal and magnetic signatures. In contrast to the host rock, the pseudotachylyte is denser, finer grained and has a different mineralogy (including equant crystals of quartz, plagioclase, pyroxene, FeTi oxides and cristobalite) which leads to the single broad melting peak at 1200–1400 °C compared to the host rock melting peaks at 1050–1250 °C and 1350–1450 °C. The vein's morphology, which undulates through the host rock, developed via viscous processes in the magma post-formation. Additionally, the pseudotachylyte has seen a strong magnetic field caused by electric currents along the fault, resulting in an isothermal remanent magnetisation which replaced the previous anhysteretic remanent magnetisation of the magma. This event also resulted in the re-locking of the Curie temperatures of the low coercive FeTi oxides.

The formation of the pseudotachylyte is considered to have been contemporaneous with repetitive LP seismicity, caused by stick-slip extrusion that persisted throughout the eruption at Soufrière Hills. Measured source duration of these events, combined with calculations of slip distances for the step-wise extrusion of magma provided the parameters required for the high velocity rotary shear experiment. The experiment demonstrated that at 10 MPa axial load (approximately 500 m depth in the conduit), 800 °C magma may be forced into the frictional melt regime in less than 15 cm of frictional sliding (in 0.15 s), thus inextricably linking drumbeat seismicity with frictional melting in the magmatic column.

SED
5, 1659–1686, 2013

Appendix A

Materials and methods

A1 Thermal measurements

Thermogravimetric measurements (TG) and low sensitivity scanning calorimetry (LS-DSC) were carried out using a Netzsch STA 449 C simultaneous thermal analysis equipment. Small chips of about 50 mg were heated in a Pt crucible (with lid) with a heating rate of 10 K min^{-1} up to 1500 °C in air. High sensitivity scanning calorimetry measurements (HS-DSC) were carried out using a Netzsch DSC 404 C. Small chips of about 25 mg were heated in a Pt crucible (with lid) with a heating rate of 10 K min^{-1} up to 1000 °C in air, cooled with 10 K min^{-1} to 100 °C and then reheated to 1000 °C.

A2 Magnetic measurements

Rock magnetic measurements were made on the Variable Field Translation Balance by Petersen Instruments at the University of Liverpool. Remanence carriers defined as low coercive materials (saturation of an isothermal remanence, IRM, below 200 mT). There are more FeTi oxides (which are the magnetic carriers) in the pseudotachylyte than in the host rock, but they are smaller, and there seems to be a tendency for higher Ti content in the magnetic carriers in the vein (5 : 1 rather than 10 : 1 Fe : Ti). A second experiment used alternating field demagnetisation of different remanent magnetisations. This experiment was run in a magnetically shielded room at LMU Munich, using the SushiBar – an automated system for paleomagnetic investigations (Wack and Gilder, 2012). First, the natural remanence NRM was measured and then demagnetised using 14 steps of increasingly higher alternating fields. Then an anhysteretic remanent magnetisation (ARM) was implied. An ARM is produced by the combination of a slowly decaying alternating field and a steady unidirectional field. For the ARM a maximum field of 90 mT was applied. This ARM was measured and then demagnetised in the

SED
5, 1659–1686, 2013

same manner as the NRM. Finally an IRM using a 1.2 T magnetic field was implied, measured and again stepwise demagnetised.

A3 Scanning electron microprobe

Uncovered thin sections of each sample were carbon coated for analysis in a CAMECA SX100 scanning electron microprobe. Backscatter electron (BSE) images (Fig. 3) highlight grain-size and density differences between the pseudotachylyte, cataclasite and host rock. Specific minerals within the samples were analysed using wavelength dispersive analysis (WDA) to verify the mineralogy identified by optical analysis.

A4 QEMSCAN

QEMSCAN analysis was completed at the Camborne School of Mines laboratory facility, University of Exeter, UK. The uncovered polished thin section was carbon coated and then scanned using the Fieldscan measurement mode, which in this case was programmed to collect an x-ray analysis every 10 µm across the sample surface in a grid (for further details see Gottlieb et al., 2000; Pirrie et al., 2004). System settings were 25 kV with a 5nA beam, and X-rays were acquired at 1000 total X-ray counts per spectrum. Resulting data (approx. 5 million data points) were processed using iDiscover software to produce customised mineral data appropriate for the sample type. This involved modifying the SIP (database) to be accurate for the sample type, assisted by the geological context of the sample. Data output included quantitative modal mineralogy, a BSE map, a full false colour mineral map and individual mineral maps for each mineral type.

A5 Tomography

3-D high-resolution tomography images were acquired through v/tome/x s 240 micro-CT scanner from GE phoenix using a high-power X-ray tube and a drx-250 rt detector system (experimental conditions: Pixel/Voxel size: 20.0 µm, 1000 images for 360° (av-

SED
5, 1659–1686, 2013

erage of 3 single images, one image skipped), exposure time of 1 s, voltage of 80 kV and current of 250 µA).

A6 Permeability

Water permeability was measured in a servo-controlled steady-state-flow permeameter at effective pressures of 5–50 MPa (Fig. 4). The effective pressure is taken as the confining pressure minus the pore fluid pressure (this assumes that the poro-elastic constant α is equal to one, see Guéguen and Palciauskas, 1994). Upstream and downstream pore fluid pressures were 9.5 MPa and 10.5 MPa, respectively (a 1 MPa pressure differential across the sample). Water permeability (κ water) was calculated during steady-state flow using Darcy's law:

$$Q/A = \kappa_{\text{water}}/\eta L(P_{\text{up}} - P_{\text{down}}) \quad \text{(A1)}$$

where Q is the volume of fluid measured per unit time, A is the cross-sectional area of the sample, η is the viscosity of the pore fluid, and L is the length of the sample.

Supplementary material related to this article is available online at http://www.solid-earth.net/5/1659/2013/sed-5-1659-2013-supplement.zip.

Acknowledgements. Thanks to A. Biggin and E. Hurst from the Geomagnetism Group at the University of Liverpool for performing the VFTB measurements. Thanks also to Alan R. Butcher (FEI) and Gavyn K. Rollinson (CSM, Exeter) for performing the QEMSCAN study and to S. Wiesmaier and D. Mueller for technical assistance. Y. Lavallée wishes to acknowledge the support of the Deutsche Forschungsgemeinschaft grant LA2191/3-1 as well as the ERC Starting Grant SLiM (306488). D. B. Dingwell wishes to acknowledge the support of a research professorship of the Bundesexzellenzinitiative (LMUexcellent) the EU funded FP7 activity 6.1 VUELCO consoritum and ERC Advanced Grant EVOKES (247076). A. Ferk and R. Leonhardt acknowledge funding by the Austrian Science foundation FWF (Grant P21221-N14).

SED
5, 1659–1686, 2013

References

Barclay, J., Rutherford, M. J., Carroll, M. R., Murphy, M. D., Devine, J. D., Gardner, J., and Sparks, R. S. J.: Experimental phase equilibria constraints on pre-eruptive storage conditions of the Soufriere Hills magma, Geophys. Res. Lett., 25, 3437–3440, 1998.

Baxter, P. J., Bonadonna, C., Dupree, R., Hards, V. L., Kohn, S. C., Murphy, M. D., Nichols, A., Nicholson, R. A., Norton, G., Searl, A., Sparks, R. S. J., and Vickers, B. P.: Cristobalite in volcanic ash of the Soufriere Hills Volcano, Montserrat, British West Indies, Science, 283, 1142–1145, 1999.

Carn, S. A., Watts, R. B., Thompson, G., and Norton, G. E.: Anatomy of a lava dome collapse: the 20 March 2000 event at Soufrière Hills Volcano, Montserrat, J. Volcanol. Geoth. Res., 131, 241–264, 2004.

Cashman, K. V., Thornber, C. R., and Pallister, J. S.: From dome to dust: shallow crystallization and fragmentation of conduit magma during the 2004–2006 dome extrusion of Mount St. Helens, Washington, in: A Volcano Rekindled: The Renewed Eruption of Mount St. Helens, 2004–2006, edited by: Sherrod, D. R., Scott, W. E., and Stauffer, P. H., Professionnal Paper 1750, US Geological Survey, 387–413, 2008.

Castro, J. M., Cordonnier, B., Tuffen, H., Tobin, M. J., Puskar, L., Martin, M. C., and Bechtel, H. A.: The role of melt-fracture degassing in defusing explosive rhyolite eruptions at volcán Chaitén, Earth Planet. Sc. Lett., 333–334, 63–69, 2012.

Cordonnier, B., Caricchi, L., Pistone, M., Castro, J., Hess, K.-U., Gottschaller, S., Manga, M., Dingwell, D. B., and Burlini, L.: The viscous-brittle transition of crystal-bearing silicic melt: direct observation of magma rupture and healing, Geology, 40, 611–614, 2012.

Curewitz, D. and Karson, J. A.: Ultracataclasis, sintering, and frictional melting in pseudotachylytes from East Greenland, J. Struct. Geol., 21, 1693–1713, 1999.

De Angelis, S.: Seismic source displacement by coda wave interferometry at Soufrière Hills Volcano, Montserrat, WI, Nat. Hazards Earth Syst. Sci., 9, 1341–1347, doi:10.5194/nhess-9-1341-2009, 2009.

De Angelis, S. and Henton, S. M.: On the feasibility of magma fracture within volcanic conduits: constraints from earthquake data and empirical modelling of magma viscosity, Geophys. Res. Lett., 38, L19310, doi:10.1029/2011GL049297, 2011.

Devine, J. D., Murphy, M. D., Rutherford, M. J., Barclay, J., Sparks, R. S. J., Carrol, M. R., Young, S. R., and Gardner, J. E.: Petroogic evidence for pre-erptive pressure-temperature

SED
5, 1659–1686, 2013

conditions, and recent reheating, of andesitic magma erupting at the soufriere Hills Volcano, Montserrat, W. I. Geophys. Res. Lett., 25, 3669–3672, 1998.
Edmonds, M. and Herd, R. A.: A volcanic degassing event at the explosive-effusive transition, Geophys. Res. Lett., 34, L21310, doi:10.1029/2007GL031379, 2007.
Ferré, E. C., Zechmeister, M. S., Geissman, J. W., MathanaSekaran, N., and Kocak, K.: The origin of high magnetic remanence in fault pseudotachylites: theoretical considerations and implication for coseismic electrical currents, Tectonophysics, 402, 125–139, 2005.
Freund, F., Salgueiro da Silva, M. A., Lau, B. W. S., Takeuchi, A., and Jones, H. H.: Electric currents along earthquake faults and the magnetization of pseudotachylite veins, Tectonophysics, 431, 131–141, 2007.
Garcia, M. and Jacobson, S.: Crystal clots, amphibole fractionation and the evolution of calc-alkaline magmas, Contributions to Mineralogy and Petrology, 69, 319–327, 1979.
Gottlieb, P., Wilkie, G., Sutherland, D., Ho-Tun, E., Suthers, S., Perera, K., Jenkins, B., Spencer, S., Butcher, A., and Rayner, J.: Using quantitative electron microscopy for process mineralogy applications, JOM, 52, 24–25, doi:10.1007/s11837-000-0126-9, 2000.
Grunewald, U., Sparks, R. S. J., Kearns, S., and Komorowski, J. C.: Friction marks on blocks from pyroclastic flows at the Soufriere Hills volcano, Montserrat: implications for flow mechanisms, Geology, 28, 827–830, 2000.
Hale, A. J. and Wadge, G.: The transition from endogenous to exogenous growth of lava domes with the development of shear bands, J. Volcanol. Geoth. Res., 171, 237–257, 2008.
Hale, A. J., Wadge, G., and Muhlhaus, H. B.: The influence of viscous and latent heating on crystal-rich magma flow in a conduit, Geophys. J. Int., 171, 1406–1429, 2007.
Harrington, R. M. and Brodsky, E. E.: Volcanic hybrid earthquakes that are brittle-failure events, Geophys. Res. Lett., 34, L06308, doi:10.1029/2006GL028714, 2007.
Harrington, R. M. and Brodsky, E. E.: Source duration scales with magnitude differently for earthquakes on the San Andreas Fault and on secondary faults in parkfield, California, B. Seismol. Soc. Am., 99, 2323–2334, 2009.
Herd, R. A., Edmonds, M., and Bass, V. A.: Catastrophic lava dome failure at Soufrière Hills Volcano, Montserrat, 12–13 July 2003, J. Volcanol. Geoth. Res., 148, 234–252, 2005.
Hirose, T. and Shimamoto, T.: Slip-weakening distance of faults during frictional melting as inferred from experimental and natural pseudotachylytes, Bull. Seismolog. Soc. Am., 95, 1666–1673, 2005.

SED
5, 1659–1686, 2013

Horwell, C., Blond, J., Michnowicz, S. K., and Cressey, G.: Cristobalite in a rhyolitic lava dome: evolution of ash hazard, Bull. Volcanol., 72, 249–253, 2010.
Horwell, C., Williamson, B., Llewellin, E., Damby, D., and Blond, J.: The nature and formation of cristobalite at the Soufrière Hills volcano, Montserrat: implications for the petrology and stability of silicic lava domes, Bull. Volcanol., 75, 1–19, 2013.
Iverson, R. M., Dzurisin, D., Gardner, C. A., Gerlach, T. M., LaHusen, R. G., Lisowski, M., Major, J. J., Malone, S. D., Messerich, J. A., Moran, S. C., Pallister, J. S., Qamar, A. I., Schilling, S. P., and Vallance, J. W.: Dynamics of seismogenic volcanic extrusion at Mount St. Helens in 2004–05. Nature, 444, 439–443, 2006.
Kendrick, J. E., Lavallée, Y., Ferk, A., Perugini, D., Leonhardt, R., and Dingwell, D. B.: Extreme frictional processes in the volcanic conduit of Mount St. Helens (USA) during the 2004–2008 eruption, J. Struct. Geol., 38, 61–76, 2012.
Kendrick, J. E., Lavallée, Y., Hess, K.-U., Heap, M. J., Gaunt, H. E., Meredith, P. G., and Dingwell, D. B.: Tracking the permeable porous network during strain-dependent magmatic flow, J. Volcanol. Geoth. Res., 260, 117–126, doi:10.1016/j.jvolgeores.2013.05.012, 2013.
Kennedy, L. A. and Russell, J. K.: Cataclastic production of volcanic ash at Mount Saint Helens, Phys. Chem. Earth, 45–46, 40–49, doi:10.1016/j.pce.2011.07.052, 2011.
Kennedy, L. A., Russell, J. K., and Nelles, E.: Origins of Mount St. Helens cataclasites: experimental insights, Am. Mineralog., 94, 995–1004, 2009.
Kim, J. W., Ree, J. H., Han, R., and Shimamoto, T.: Experimental evidence for the simultaneous formation of pseudotachylyte and mylonite in the brittle regime, Geology, 38, 1143–1146, 2010.
Kirkpatrick, J. D. and Rowe, C. D.: Disappearing ink: how pseudotachylytes are lost from the rock record, J. Struct. Geol., 52, 183–198, 2013.
Lavallée, Y., Meredith, P. G., Dingwell, D. B., Hess, K. U., Wassermann, J., Cordonnier, B., Gerik, A., and Kruhl, J. H.: Seismogenic lavas and explosive eruption forecasting, Nature, 453, 507–510, 2008.
Lavallée, Y., Mitchell, T. M., Heap, M. J., Vasseur, J., Hess, K.-U., Hirose, T., and Dingwell, D. B.: Experimental generation of volcanic pseudotachylytes: constraining rheology, J. Struct. Geol., 38, 222–233, 2012a.
Lavallée, Y., Varley, N., Alatorre-Ibargüengoitia, M., Hess, K. U., Kueppers, U., Mueller, S., Richard, D., Scheu, B., Spieler, O., and Dingwell, D.: Magmatic architecture of dome-building eruptions at Volcán de Colima, Mexico, Bull. Volcanol., 74, 249–260, 2012b.

SED
5, 1659–1686, 2013

Lavallée, Y., Benson, P., Hess, K.-U., Flaws, A., Schillinger, B., Meredith, P. G., and Dingwell, D. B.: Reconstructing magma failure and the permeable degassing network, Geology, 41, 515–518, doi:10.1130/G33948.1, 2013.

Lensky, N. G., Sparks, R. S. J., Navon, O., and Lyakhovsky, V.: Cyclic activity at Soufrière Hills Volcano, Montserrat: degassing-induced pressurization and stick-slip extrusion, Special Publications, 307, Geological Society, London, 169–188, 2008.

Lin, A. M.: Injection veins of crushing-originated pseudotachylyte and fault gouge formed during seismic faulting, Eng. Geol., 43, 213–224, 1996.

Luckett, R., Loughlin, S., De Angelis, S., and Ryan, G.: Volcanic seismicity at Montserrat, a comparison between the 2005 dome growth episode and earlier dome growth, J. Volcanol. Geoth. Res., 177, 894–902, 2008.

Magloughlin, J. F. and Spray, J. G.: Frictional Melting Processes and Products in Geological Materials, Science Direct, 141 pp., 1992.

Melnik, O. E. and Sparks, R. S. J.: Dynamics of magma ascent and lava extrusion at the Soufrière Hills Volcano, Montserrat, in: The Eruption of the Soufrière Hills Volcano, Montserrat from 1995 to 1999, edited by: Kokelaar, T. D. B., Geological Society, London, 153–172, 2002.

Murphy, M. D., Sparks, R. S. J., Barclay, J., Carroll, M. R., and Brewer, T. S.: Remobilization of andesite magma by intrusion of mafic magma at the Soufriere Hills Volcano, Montserrat, West Indies, J. Petrol., 41, 21–42, 2000.

Neuberg, J., Baptie, B., Luckett, R., and Stewart, R.: Results from the broadband seismic network on Montserrat, Geophys. Res. Lett., 25, 3661–3664, 1998.

Neuberg, J., Tuffen, H., Collier, L., Green, D., Powell, T., and Dingwell, D.: The trigger mechanism of low-frequency earthquakes on Montserrat, J. Volcanol. Geoth. Res., 153, 37–50, 2006.

Okumura, S., Nakamura, M., Nakano, T., Uesugi, K., and Tsuchiyama, A.: Shear deformation experiments on vesicular rhyolite: Implications for brittle fracturing, degassing, and compaction of magmas in volcanic conduits, J. Geophys. Res., 115, B06201, doi:10.1029/2009JB006904, 2010.

Pirrie, D., Butcher, A. R., Power, M. R., Gottlieb, P., and Miller, G. L.: Rapid quantitative mineral and phase analysis using automated scanning electron microscopy (QEMSCAN); potential applications in forensic geoscience, Geological Society Special Publication, London, 2004.

SED
5, 1659–1686, 2013

Plail, M., Edmonds, M., Barclay, J., Humphreys, M. C. S., and Herd, R.: Geochemical evidence for relict degassing pathways preserved in andesite, Earth Planet. Sc. Lett., in review, 2013.
Rowe, C. A., Thurber, C. H., and White, R. A.: Dome growth behavior at Soufriere Hills Volcano, Montserrat, revealed by relocation of volcanic event swarms, 1995–1996, J. Volcanol. Geoth. Res., 134, 199–221, 2004.
Rowe, C. D., Moore, J. C., Meneghini, F., and McKeirnan, A. W.: Large-scale pseudotachylytes and fluidized cataclasites from an ancient subduction thrust fault, Geology, 33, 937–940, 2005.
Rutherford, M. J. and Devine, J. D.: Magmatic conditions and magma ascent as indicated by hornblende phase equilibria and reactions in the 1995–2002 Soufriere Hills Magma, J. Petrol., 44, 1433–1453, 2003.
Sosman, R. B.: The Phases of Silica, Rutgers University Press, New Brunswick, N. J., 389 pp., 1965.
Spray, J. G.: Frictional melting processes in planetary materials: from hypervelocity impact to earthquakes, Ann. Rev. Earth Planet. Sci., 38, 221–254, 2010.
Tuffen, H. and Dingwell, D.: Fault textures in volcanic conduits: evidence for seismic trigger mechanisms during silicic eruptions, Bull. Volcanol., 67, 370–387, 2005.
Voight, B. and Elsworth, D.: Instability and collapse of hazardous gas-pressurized lava domes, Geophys. Res. Lett., 27, 1–4, 2000.
Voight, B., Sparks, R. S., Miller, A. D., Stewart, R. C., Hoblitt, R. P., Clarke, A., Ewart, J., Aspinall, W. P., Baptie, B., Calder, E. S., Cole, P., Druitt, T. H., Hartford, C., Herd, R. A., Jackson, P., Lejeune, A. M., Lockhart, A. B., Loughlin, S. C., Luckett, R., Lynch, L., Norton, G. E., Robertson, R., Watson, I. M., Watts, R., and Young, S. R.: Magma flow instability and cyclic activity at Soufriere Hills Volcano, Montserrat, British West Indies, Science, 283, 1138–1142, 1999.
Watts, R. B., Herd, R. A., Sparks, R. S., and Young, S. R.: Growth patterns and emplacement of the andesitic lava dome at Soufriere Hills volcano, in: The Eruption of Soufriere Hills Volcano, Montserrat, from 1995 to 1999, edited by: Druitt, T. H. and Kokelaar, B. P., Geological Society of London Memoirs, 115–152, 2002.
Zellmer, G. F., Hawkesworth, C. J., Sparks, R. S. J., Thomas, L. E., Harford, C. L., Brewer, T. S., and Loughlin, S. C.: Geochemical evolution of the Soufrière Hills Volcano, Montserrat, Lesser Antilles Volcanic Arc, J. Petrol., 44, 1349–1374, 2003.

SED
5, 1659–1686, 2013

Fig. 1. Field photo of the shear band. Aphantic pseudotachylyte layers of the shear band are interspersed with cataclastic layers and lenses. Photograph illustrates the lateral variation in thickness and its morphology, which suggests formation in viscous magma in the conduit.

SED
5, 1659–1686, 2013

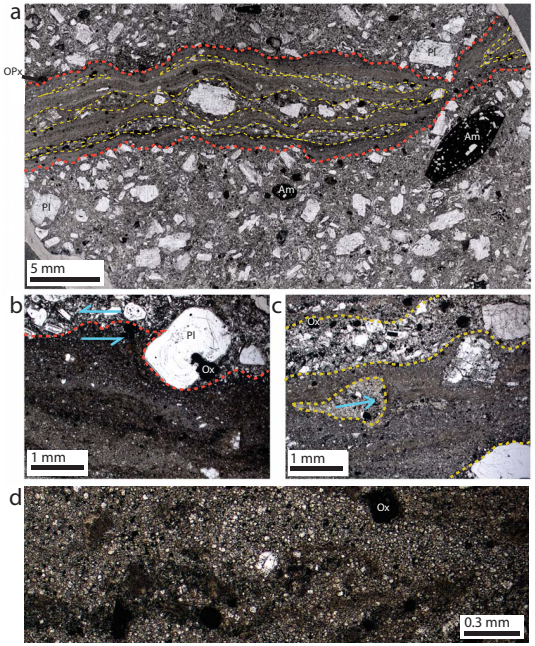

Fig. 2. Photomicrographs of the shear band. **(a)** A wide view of pseudotachylyte (dark grey) and cataclasite (grey) layers in the shear band cutting through the andesite host rock, containing plagioclase, amphibole pseudomorphs (replaced by reaction products), pyroxene and FeTi oxides. Morphology of the vein shows shear band pinching out and lenses of cataclasites between pseudotachylyte veins of more constant thickness. **(b)** Inferred shear direction from flow morphology of the pseudotachylyte around a host-rock phenocryst at the vein boundary. **(c)** Cataclastic lens hosted in a pseudotachylyte layer with bulbous onset and elongate tail indicating flow direction of the band. **(d)** Internal structure in the pseudotachylyte–cataclasite interface indicating turbulent flow. Red dashed lines mark the boundary of the shear band, yellow dashed lines show boundaries between pseudotachylyte and cataclasites, arrows represent inferred flow/shear directions.

SED
5, 1659–1686, 2013

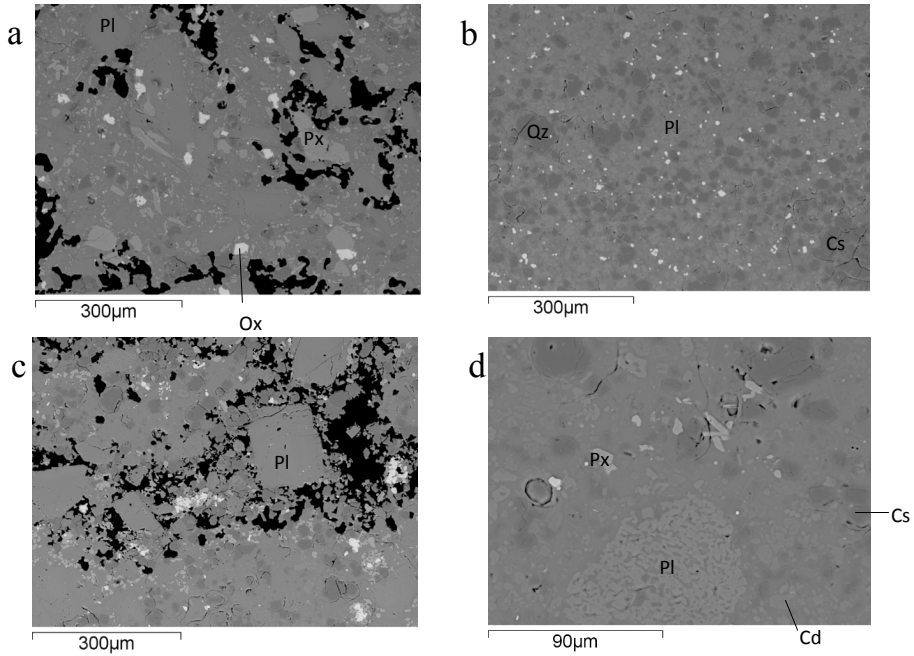

Fig. 3. Backscatter electron (BSE) images of the sample. **(a)** Host rock, **(b)** pseudotachylyte, **(c)** cataclasite and **(d)** sieve textured plagioclase in the pseudotachylyte. Here Qz = quartz, Pl = plagioclase, Px = pyroxene, Ox = FeTi oxide, Cd = cordierite and Cs = cristobalite.

SED
5, 1659–1686, 2013

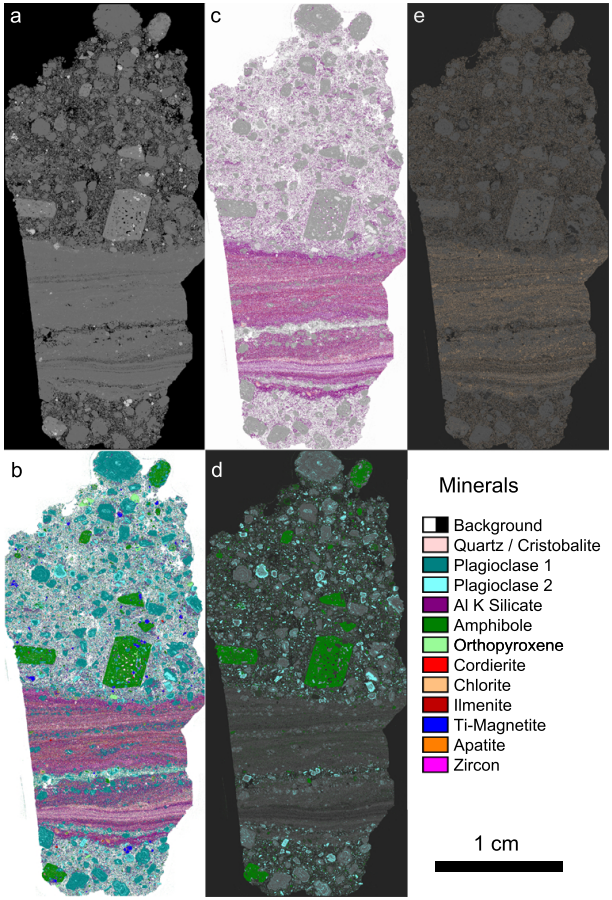

Fig. 4. Distribution of minerals using QEMSCAN. **(a)** BSE image of the thin section used for analysis, including host rock, cataclasite and pseudotachylyte **(b)** composite of all resolved minerals and porosity in white **(c)** distribution of Al K silicate (potentially orthoclase) and cordierite with other minerals in greyscale and porosity in white **(d, e)**.

SED
5, 1659–1686, 2013

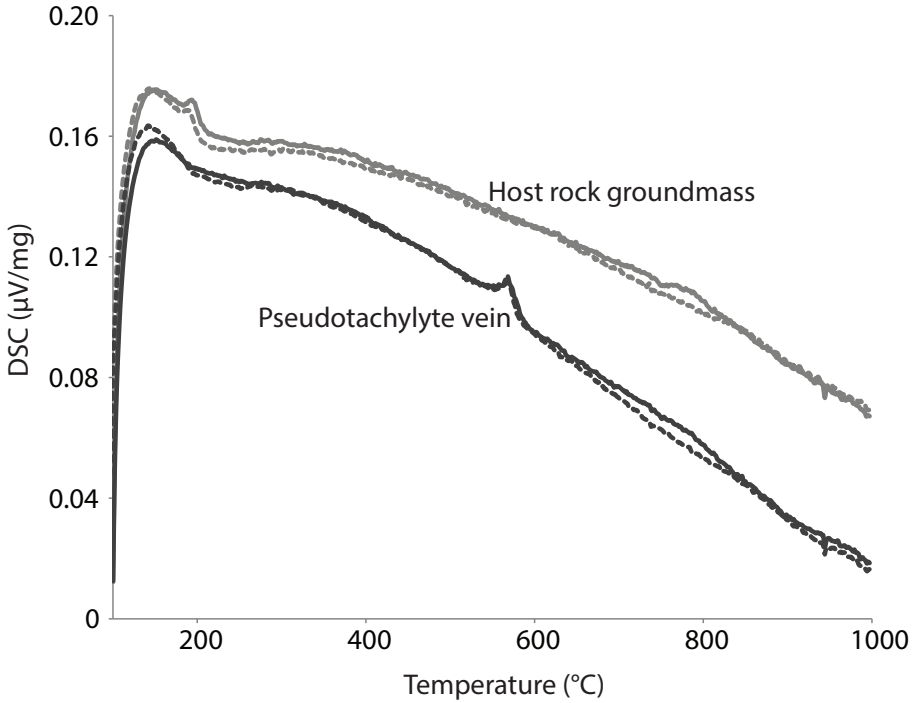

Fig. 5. Thermal measurements by high sensitivity differential scanning calorimetry (HS-DSC). Measurements were carried out using a Netzsch DSC 404 C. A sharp endothermic peak at about 190 °C in the host rock (light grey trace) corresponds to a critobalite $\alpha - \beta$ phase transition and the trace shows no evidence of a potential glassy phase. An endothermic peak at about 570 °C corresponding to the $\alpha - \beta$ phase transition in quartz is seen in the pseudotachylyte vein (dark grey trace). The same exothermic peaks are visible on the second run of the experiments with the same sample confirming their respective phase transitions (dashed lines).

SED
5, 1659–1686, 2013

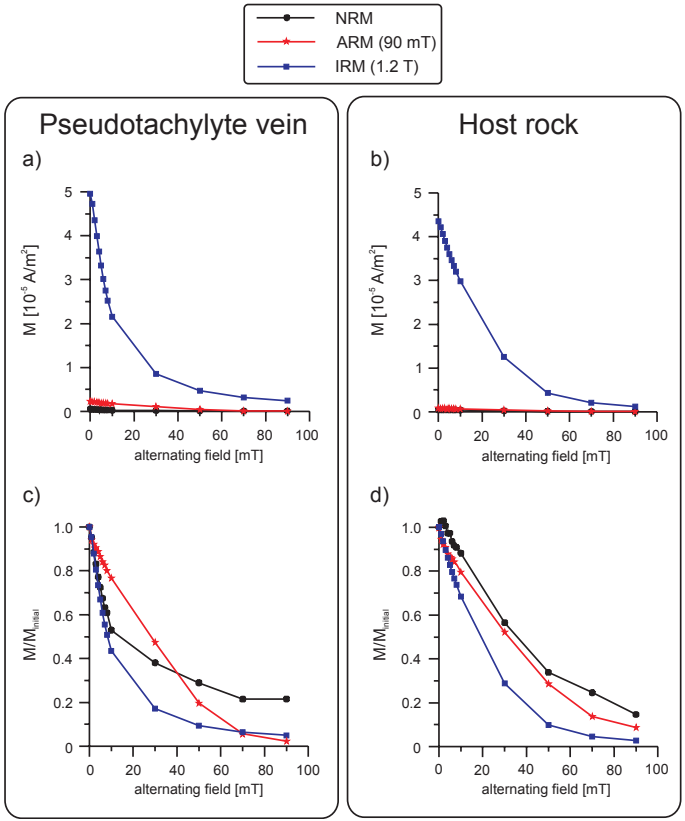

Fig. 6. Rock magnetic measurements. Alternating field demagnetisations of NRM, ARM and IRM of pseudotachylyte and host rock. Shown are first **(a, b)** magnetisation vs. alternating field, then **(c, d)** normalised magnetisation (normalisation using initial magnetisation at 0 mT alternating field) vs. alternating field. NRM of the pseudotachylyte is analogue to an IRM while the NRM of the host rock is analogue to an ARM.

SED
5, 1659–1686, 2013

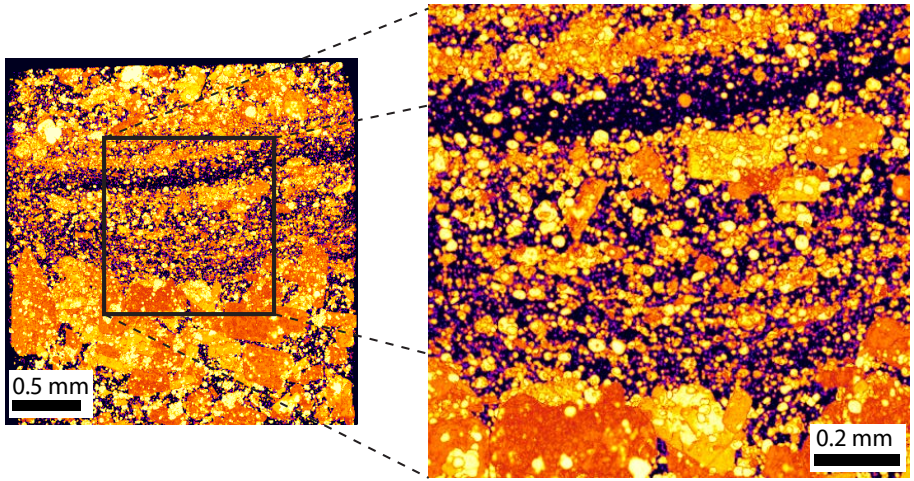

Fig. 7. Stacked image of crystals in 3-D. All crystals in the sample, at a voxel size of 20 µm (approximate detection limit 40 µm) flattened into a slice. The figure shows heavier elements in brighter colours, and clearly illustrates the very fine grained nature of the pseudotachylyte vein (majority of crystals below detection-size and are not resolved).

SED
5, 1659–1686, 2013

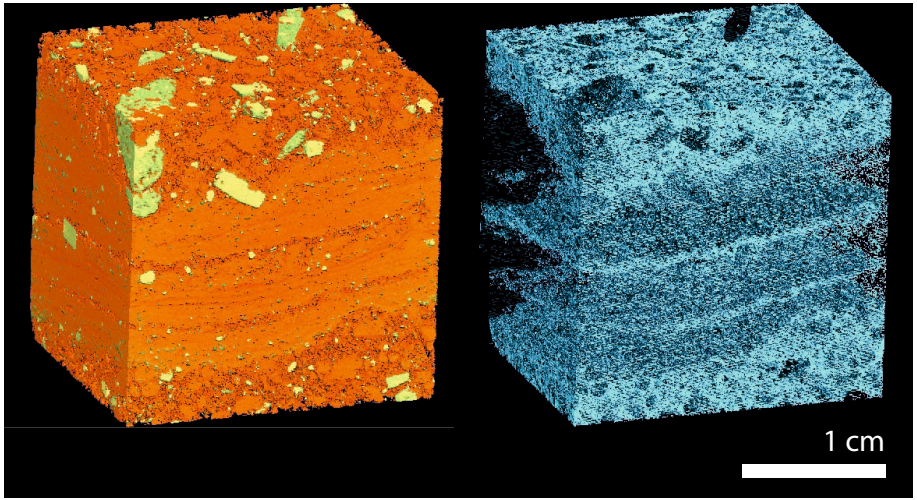

Fig. 8. Tomography of the shear band in the host rock. Solid fraction of the sample is shown in yellow (oxides and pyroxenes) and orange (plagioclase and groundmass) according to density. A 3-D reconstruction of the pore space is shown in blue, highlighting the negligible porosity of the pseudotachylyte layers and its influence on the permeable porous network.

SED
5, 1659–1686, 2013

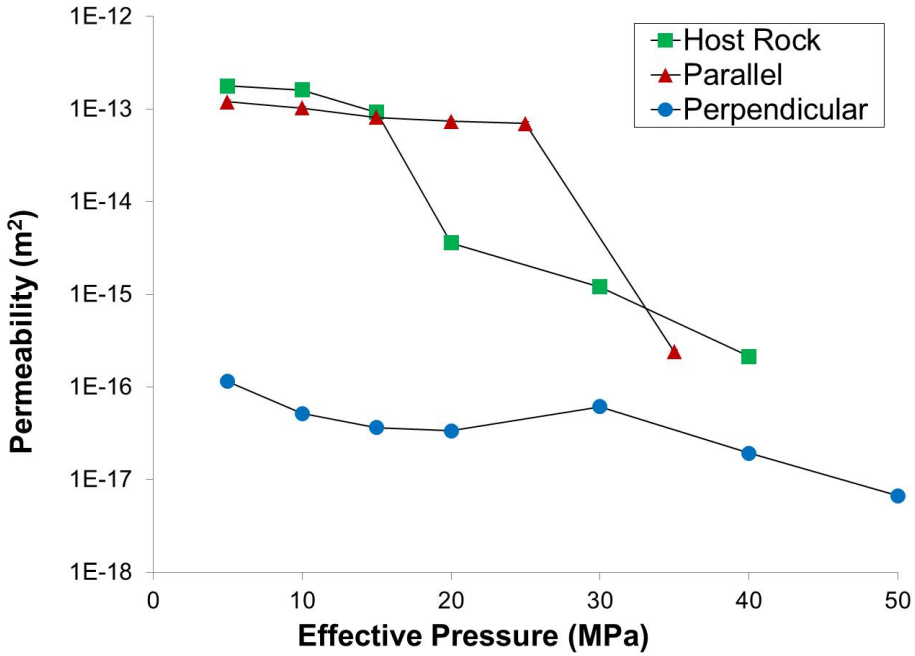

Fig. 9. Permeability evolution. Steady-state water permeability measured at effective pressures of 5–50 MPa for sample cores (2.5 cm diameter) with no shear band (host rock), and drilled parallel and perpendicular to the pseudotachylyte-bearing shear band. When the pseudotachylyte is parallel to flow, the flow rate is still controlled by the host rock, but when the vein runs perpendicular to flow it controls the permeability, which is drastically reduced. Additionally permeability is reduced as effective pressure is increased and cracks are slowly closed, this effect is less apparent in the perpendicular-cut sample as the porosity of the pseudotachylyte is already negligible.

SED
5, 1659–1686, 2013

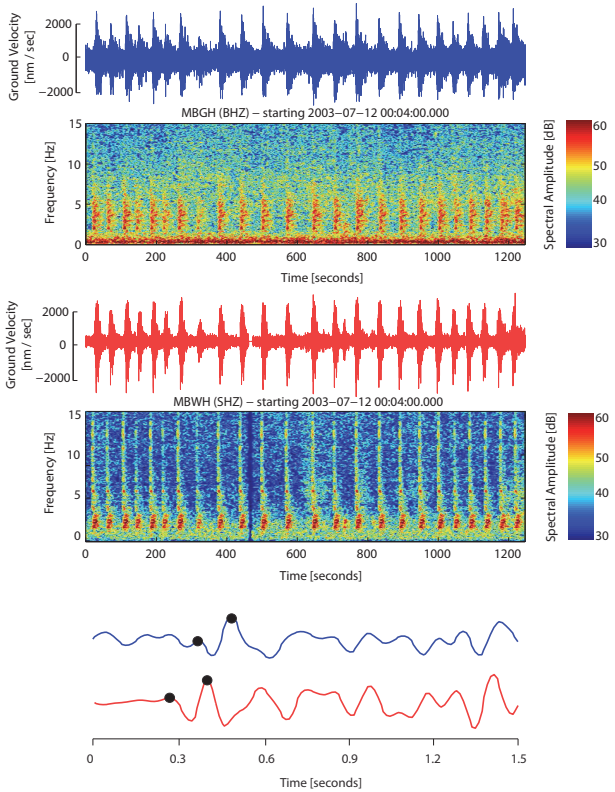

Fig. 10. Repetitive seismicity at Soufrière Hills volcano. Seismograms for 18 min of repeating earthquakes at stations MBGH and MBWH recorded on 12 July 2003 approximately 12 h before the largest dome collapse in SHV history. Bottom Panel: the black dots highlight the width of a single *P* wave pulse from the seismograms above, which provide an estimate of source duration.

SED
5, 1659–1686, 2013

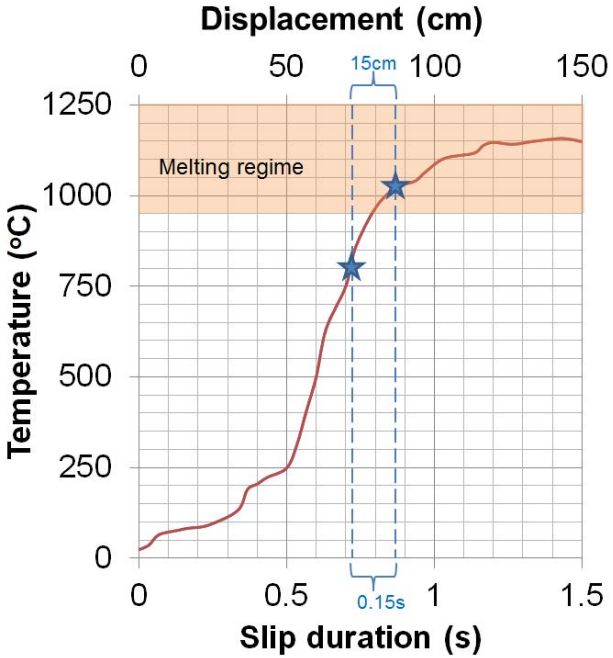

Fig. 11. Frictional melting of SHV andesite using a high velocity rotary shear apparatus. Increasing temperature with time and slip distance at 10 MPa axial load and 1.0 m s^{-1} slip velocity. Starting from room temperature melting is achieved in 0.75 s (75 cm). The blue stars represent the change in temperature that results from a slip episode of 15 cm in 0.15 s (displacement parameters calculated from the seismic events at SHV in Fig. 10) from a starting magmatic temperature of 800 °C, where the magma temperature is increased by friction to 1025 °C in that interval, with the onset of melting occurring at approximately 950 °C (see also Supplement).

SED
5, 1659–1686, 2013